

# Antagonizing CD105 and androgen receptor to target stromal-epithelial interactions for clinical benefit

Bethany N. Smith,<sup>1</sup> Rajeev Mishra,<sup>1,2</sup> Sandrine Billet,<sup>1</sup> Veronica R. Placencio-Hickok,<sup>1</sup> Minhyung Kim,<sup>3</sup> Le Zhang,<sup>1</sup> Frank Duong,<sup>1</sup> Anisha Madhav,<sup>1</sup> Kevin Scher,<sup>1</sup> Nancy Moldawer,<sup>1</sup> Amy Oppenheim,<sup>1</sup> Bryan Angara,<sup>1,4</sup> Sungyong You,<sup>3</sup> Mourad Tighiouart,<sup>1</sup> Edwin M. Posadas,<sup>1</sup> and Neil A. Bhowmick<sup>1,4</sup>

<sup>1</sup>Department of Medicine, Cedars-Sinai Cancer, Los Angeles, CA 90048, USA; <sup>2</sup>School of Life Sciences & Biotechnology, Chhatrapati Shahu Ji Maharaj University, Kanpur, Uttar Pradesh 208024, India; <sup>3</sup>Department of Surgery, Cedars-Sinai Cancer, Los Angeles, CA 90048, USA; <sup>4</sup>VA Greater Los Angeles Healthcare System, Los Angeles, CA 90073, USA

**Androgen receptor signaling inhibitors (ARSIs) are standard of care for advanced prostate cancer (PCa) patients. Eventual resistance to ARSIs can include the expression of androgen receptor (AR) splice variant, AR-V7, expression as a recognized means of ligand-independent androgen signaling. We demonstrated that interleukin (IL)-6-mediated AR-V7 expression requires bone morphogenic protein (BMP) and CD105 receptor activity in both PCa and associated fibroblasts. Chromatin immunoprecipitation supported CD105-dependent ID1- and E2F-mediated expression of RBM38. Further, RNA immune precipitation demonstrated RBM38 binds the AR-cryptic exon 3 to enable AR-V7 generation. The forced expression of AR-V7 by primary prostatic fibroblasts diminished PCa sensitivity to ARSI. Conversely, downregulation of AR-V7 expression in cancer epithelia and associated fibroblasts was achieved by a CD105-neutralizing antibody, carotuximab. These compelling pre-clinical findings initiated an interventional study in PCa patients developing ARSI resistance. The combination of carotuximab and ARSI (i.e., enzalutamide or abiraterone) provided disease stabilization in four of nine assessable ARSI-refractory patients. Circulating tumor cell evaluation showed AR-V7 downregulation in the responsive subjects on combination treatment and revealed a three-gene panel that was predictive of response. The systemic antagonism of BMP/CD105 signaling can support ARSI re-sensitization in pre-clinical models and subjects that have otherwise developed resistance due to AR-V7 expression.**

## INTRODUCTION

Prostate cancer (PCa) continues to be the second leading cause of cancer-related death in men.<sup>1</sup> It represents more than one in five new cancer diagnoses, with an increase in metastatic progression over the last decade.<sup>2</sup> For men who do not have localized disease amenable to focal therapies such as surgery or radiation therapy, androgen signaling axis targeting is the primary systemic strategy employed. While androgen receptor signaling inhibitors (ARSI; e.g., abiraterone acetate, enzalutamide, bicalutamide, and apalutamide)

are initially effective, the development of resistance is an unfortunate reality for many patients. Multiple mechanisms, such as androgen receptor (AR) amplification, activating mutations, deletions, gene fusions, and RNA splice variants, have been associated with the emergence of ARSI resistance.<sup>3,4</sup> The latter results in truncations of AR due to RNA splicing events that lack the androgen-binding domain to enable ligand-independent androgen signaling and resistance to ARSI therapy. Here, we explored the mechanism of splicing of the particularly well-studied AR splice variant-7 (AR-V7), which has an insertion of a cryptic exon 3 resulting in a premature transcriptional stop.<sup>5</sup> AR-V7 can transactivate androgen-responsive elements on DNA alone or in combination with full-length AR in a ligand-independent manner.<sup>4,6-8</sup> However, castration-resistant PCa (CRPC) is not necessarily a cell-autonomous event.<sup>9-14</sup> Our findings suggest AR-V7 has a role in prostatic carcinoma-associated fibroblasts (CAFs).

The designation of CAF in our studies is based on the biological capacity to induce nontumorigenic BPH1 cells to generate tumors, as opposed to the normal associated fibroblasts (NAFs), which do not have this capacity.<sup>15,16</sup> Transforming growth factor  $\beta$  (TGF- $\beta$ ) signaling is widely recognized as a regulator of PCa development, progression, and castration resistance.<sup>11,17</sup> TGF- $\beta$  was initially identified to be elevated in response to castration and found to be a determinant of PCa epithelial cell death.<sup>18,19</sup> We have reported that inhibition of TGF- $\beta$  signaling through epigenetic silencing of TGF- $\beta$  receptor type 2 (*Tgfr2*) in prostatic CAF potentiates tumor progression and castrate resistance through paracrine signaling mechanisms.<sup>9,11,12,14,20</sup> An alternative mechanism for limiting TGF- $\beta$  signaling is by the expression of CD105 (endoglin, ENG), a TGF- $\beta$  family coreceptor. Importantly, CD105 simultaneously inhibits TGF- $\beta$  signaling while promoting

Received 14 April 2022; accepted 25 August 2022;  
<https://doi.org/10.1016/j.ymthe.2022.08.019>

**Correspondence:** Neil A. Bhowmick, Department of Medicine, Cedars-Sinai Cancer, Los Angeles, CA 90048, USA

**E-mail:** [bhowmickn@cshs.org](mailto:bhowmickn@cshs.org)

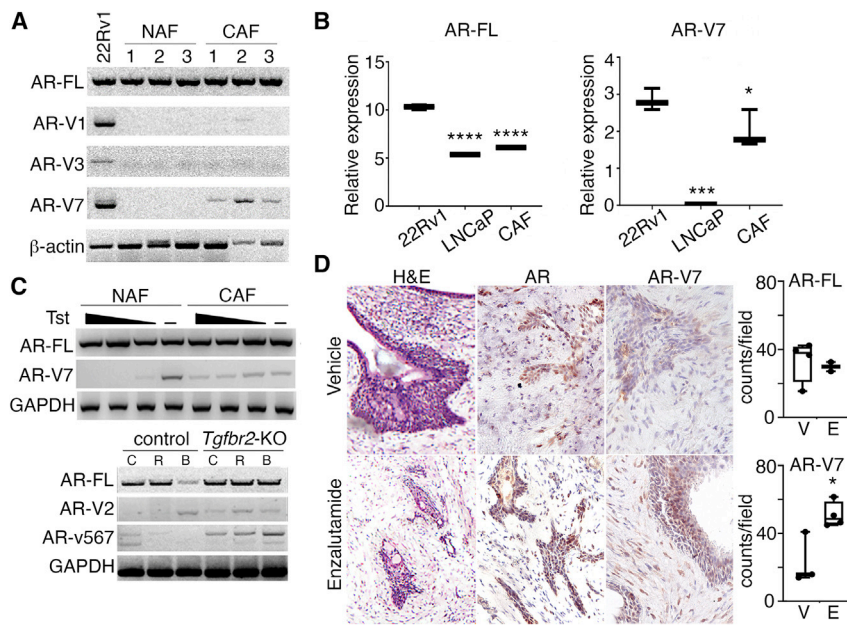


**Figure 1. AR-variant expression in PCa epithelia and prostate fibroblasts**

(A and B) Full-length AR (AR-FL) and splice variant mRNA expression in human PCa cell lines (22Rv1, LNCaP) and primary human prostatic fibroblasts (NAF and CAF) were evaluated by RT-PCR.  $\beta$ -actin or GAPDH were used as a loading control for RT-PCR gels and qPCR analyses ( $n \geq 6$ ). (C) mRNA expression in NAF and CAF were measured following culturing with dihydroxytestosterone (Tst; 10, 5, 2.5, 0 nM) for 14 days. AR-FL, AR-V2, and ARv567es mRNA expression in *Tgfr2*<sup>fllox/fllox</sup> (control) and *Tgfr2*<sup>ispKO</sup> (*Tgfr2*-KO) mouse prostatic fibroblasts treated with R1881 (R, 10 nM), bicalutamide (B, 10  $\mu$ M), or DMSO (C, control) for 48 h. (D) Hematoxylin and eosin (H&E) histological staining, immunohistochemical localization of AR, and AR-V7 expression was localized in PDX from mice treated with vehicle (V) or enzalutamide (E; 40 mg/kg) for 4 days ( $n \geq 4$ ). Nuclei were counterstained with hematoxylin and scale bar represents 30  $\mu$ m. Data were analyzed using one-tailed t test, where statistical significance was indicated: \* $p < 0.05$ , \*\*\* $p < 0.001$ , and \*\*\*\* $p < 0.0001$ .

bone morphogenic protein (BMP) downstream signal transduction.<sup>21</sup> As such, CD105 inhibits SMAD2 and SMAD3 activity while promoting SMAD1 and SMAD5 signaling and the downstream canonical inhibitor of differentiation family of transcription factors (ID1, ID2, ID3, ID4).<sup>22</sup> CD105 expression in proliferating endothelia during embryonic development implicated its role in tumor neovasculture formation.<sup>23</sup> However, antagonizing CD105/BMP signaling, without activating TGF- $\beta$  signaling,<sup>24</sup> by a specific neutralizing antibody (carotuximab) has shown limited clinical benefit as an anti-angiogenic.<sup>25,26</sup> Beyond endothelial biology, CD105 is expressed by cancer epithelia, immune cells, and fibroblasts.<sup>12,27,28</sup> Unfortunately, single-agent carotuximab had limited therapeutic benefit in mouse models and in patients with CRPC.<sup>12,25</sup> Stemming from the observation that ARSI promoted CD105 upregulation by both PCa epithelia and CAF,<sup>12</sup> we found carotuximab in combination with castration or enzalutamide treatment significantly reduced tumor progression in mouse models of CRPC. We found that the AR-V7 expression was dependent on CD105 in both PCa epithelia and stromal fibroblasts. Our data extend previous studies of positive regulation of AR splicing by interleukin (IL)-6,<sup>29–31</sup> to include a novel mechanism involving CD105-mediated RNA-binding protein activity in PCa epithelial and fibroblast cells.

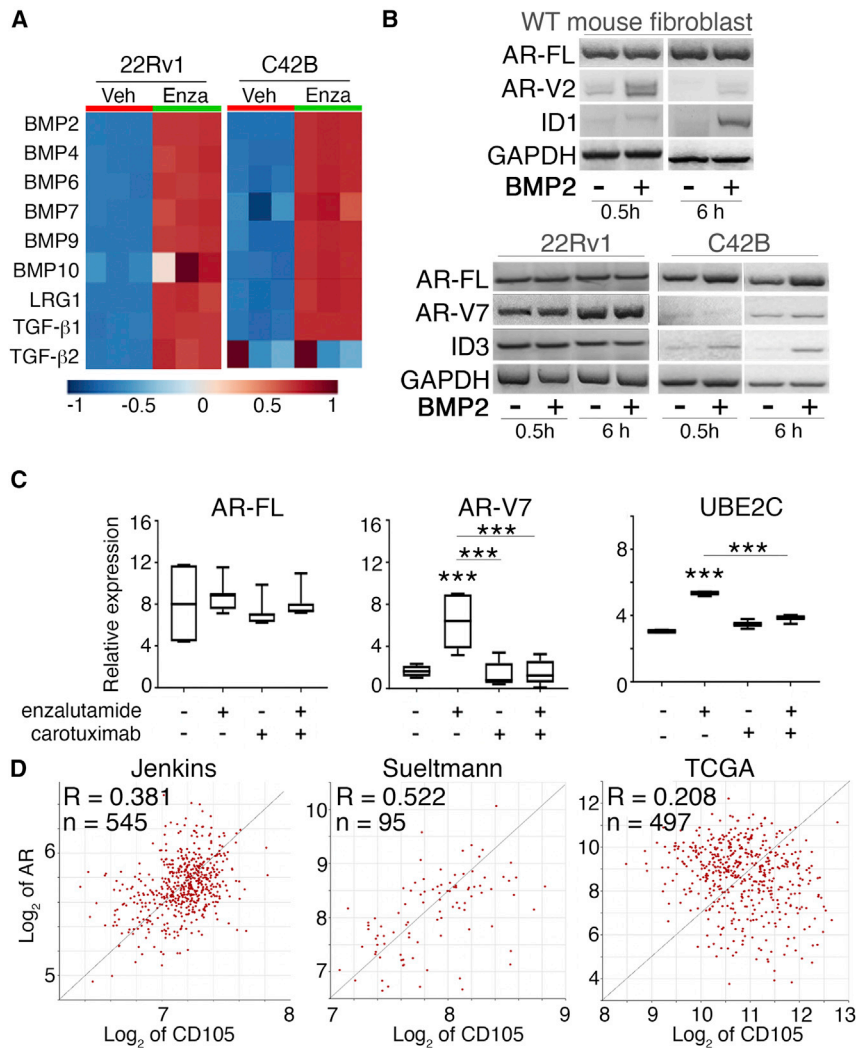
Despite the importance of targeting androgen signaling, the efficacy of available ARSIs is limited with patients continuing to progress through treatment. Chemotherapy (e.g., taxane and platinum) remains standard of care for subjects developing resistance to ARSIs, but associated toxicity can be undesirable to many patients.<sup>32,33</sup> The introduction of radionuclide and antibody-directed radio-conjugates also bears consideration for patients with CRPC who have progressed on ARSIs, but their impact may be limited due to dosing restrictions.<sup>34,35</sup> The pre-clinical findings here were followed by combina-

tion therapy of carotuximab and enzalutamide or abiraterone in metastatic CRPC patients, which suggested a viable alternative to chemotherapy for those subjects on ARSI therapy.

## RESULTS

### AR splice variant expression in PCa epithelia and associated fibroblasts

Patients that express AR-V7 in circulating tumor cells are reported to have a worse progression-free survival (PFS) and overall survival compared with those that do not have detectable AR-V7 expression.<sup>36</sup> Based on the understanding that both PCa epithelia and CAF express AR, we explored the possibility aberrant AR splice variant expression in prostatic fibroblastic cells. Full-length AR was similarly expressed in three independent, primary human NAF and CAF cells generated from prostatectomy tissues (Figure 1A). The NAF lines had undetectable expression of the AR variants; however, AR-V7 was prominently expressed by CAFs compared with 22Rv1 cells (Figure S1A). The expression of AR-V7 is rare in primary PCa tumors, but it is expressed in patients with metastatic disease progressing through ARSI treatment.<sup>37</sup> To provide context, AR full-length expression in NAF and CAF was comparable with that found in LNCaP cells, but significantly less than that in CWR22Rv1 (22Rv1) PCa cell lines cells ( $p < 0.0001$ ; Figure 1B). While AR-V7 expression in CAF lines was less than that in 22Rv1 ( $p < 0.05$ ), it was greater than the negligible expression found in LNCaP cells ( $p < 0.001$ ). 22Rv1 also expressed AR-V1 and AR-V3; these two AR variants were largely absent in the prostatic fibroblastic cells, except for weak expression of AR-V1 in one CAF line. As the prostatic fibroblasts were generated and maintained at  $10 \times 10^{-5}$  M testosterone, we tested the effect of testosterone reduction for 2 weeks and found that the expression of AR-V7 was upregulated in the NAF under  $2.5 \times 10^{-5}$  M testosterone and further



induced in testosterone-free medium (Figure 1C). The expression of AR-V7 was greater in CAF than in NAF in testosterone-free conditions.

In light of elevated TGF- $\beta$  expression under castrate conditions,<sup>18</sup> it was important to explore the impact on stromal TGF- $\beta$  signaling when ARSI are used to target PCa. We found that the expression of AR full length was similar in mouse primary prostatic fibroblasts generated from *Tgfr2*<sup>flax/flax</sup> (control) and *Tgfr2*<sup>fspKO</sup> (*Tgfr2* knockout [*Tgfr2*-KO]) mice (Figure 1C). As a point of clarification, unlike the heterogeneity in the loss of *Tgfr2* expression of the fibroblasts of the *Tgfr2*<sup>fspKO</sup> mice, the *Tgfr2*-KO fibroblasts cultured from the prostates of these mice are homogeneously knockout for *Tgfr2*.<sup>20</sup> However, the *Tgfr2*-KO primary fibroblasts expressed greater levels of AR splice variant, AR-V2 (ortholog of human AR-V7) mRNA compared with control fibroblasts under basal conditions. Protein levels of AR (110 kDa) and AR variants (75–100 kDa) were also elevated in *Tgfr2*-KO fibroblasts compared

### Figure 2. CD105 antagonism regulates AR-variant expression in PCa cells

(A) Heatmap of TGF- $\beta$  and BMP family ligand expression by 22Rv1 and C4-2B PCa cell lines treated with enzalutamide or vehicle for 72 h (two-way ANOVA,  $p < 0.0001$ ). (B) mRNA expression of AR-FL and AR-V7 was measured in prostatic fibroblasts and PCa cells treated with BMP-2 for 0.5 or 6 h. (C) AR-FL, AR-V7, and UBE2C mRNA expression was measured in 22Rv1 cells treated with enzalutamide, carotuximab, and its combination, or vehicle for 72 h under 2% O<sub>2</sub>. (D) Correlation between AR and CD105 mRNA expression was determined in three indicated datasets ( $R^2$ ). Enzalutamide was used at 5  $\mu$ M; BMP-2 10 ng/mL; carotuximab 10  $\mu$ g/mL; DMSO used as vehicle control. For qPCR data, GAPDH was used as loading control and data analyzed using two-tailed t test, where statistical significance was indicated: \*\*\* $p < 0.001$  and \*\*\*\* $p < 0.0001$ .

with control (Figure S1B). AR antagonism by bicalutamide elevated AR-V2 expression in both control and *Tgfr2*-KO fibroblasts over basal levels. Next, we compared AR full-length and AR-V7 expression in patient-derived xenografts (PDXs) by immunohistochemistry (Figure 1D). As previously reported, the expression of AR-V7 was elevated in tumor epithelia after the mice were treated with enzalutamide (AR antagonist) for 4 days. Strikingly, fibroblastic AR-V7 expression was observed to be elevated ( $p = 0.0238$ ) following enzalutamide treatment, with little change in AR expression levels. Knockout of *Tgfr2* did not significantly change cell-surface expression of CD105, determined by flow cytometry (Figure S1C). However, TGF- $\beta$  signaling inhibition and increased CD105 was

found in both epithelial and fibroblastic cells by enzalutamide treatment, in agreement with previous studies (Figure S1D).<sup>12,38</sup> Since inhibition of TGF- $\beta$  signaling via knockout of *Tgfr2* was associated with increased AR-V7 expression, we reasoned that the expression of CD105 could have a similar result in epithelial and fibroblastic cells. In the context of ARSIs, CD105 induction could contribute to AR-V7 expression.

To better understand CD105 downstream signaling, we initially quantitated the expression of TGF- $\beta$  and BMP ligands by PCa epithelial lines, C4-2B and 22Rv1. Nearly all TGF- $\beta$  and BMP ligand mRNAs examined were found to be upregulated by enzalutamide treatment in both PCa cell lines, except TGF- $\beta$ 2 in C4-2B cells (-ANOVA  $p < 0.0001$ ; Figure 2A). BMP2 promoted AR-FL ( $p < 0.0001$ ) and AR-V7 ( $p < 0.0001$ ) expression, respectively in C4-2B (Figure 2B). BMP2 respectively upregulated ID1 and ID3 in wild-type fibroblasts and C4-2B cells, respectively within 30 min compared with vehicle treatment under serum-free conditions.

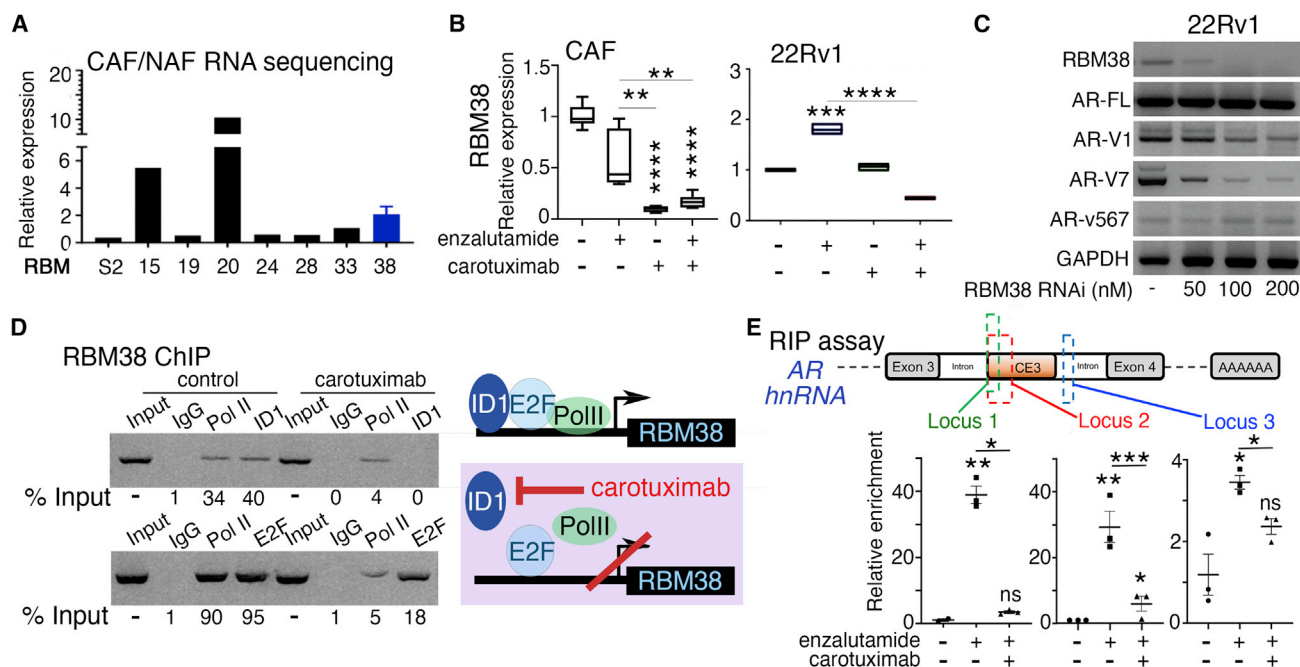


**Figure 3. CD105 and RBM38 signaling in PCa cells**

(A) RNA-binding motif expression by primary human prostatic fibroblast RNA sequencing analysis from Kato et al.<sup>12</sup> was analyzed. Data represents expression of genes as a ratio of CAF/NAF. (B) RBM38 mRNA expression was measured in prostatic CAF and 22Rv1 treated with enzalutamide (5  $\mu$ M), carotuximab (10  $\mu$ g/mL), or the combination, or vehicle for 72 h under 2% O<sub>2</sub>. (C) AR-FL, AR-V1, AR-V7, and AR-v567es mRNA expression was measured in 22Rv1 following RBM38 siRNA for 48 h. (D) RBM38 promoter ChIP analysis examined the enrichment of RNA polymerase II (Pol II), ID1, and E2F1 in 22Rv1 cells treated with carotuximab or IgG control. A representative gel image is shown with densitometric analysis of enrichment as a percentage of input. Model of the role of ID1 at RBM38 promoter. ID1 recruitment at RBM38 promoter enables RNA polymerase II loading, whereas CD105 inhibition by carotuximab blocks both ID1 and RNA polymerase II. E2F recruitment to the RBM38 promoter is not dependent on ID1 loading. (E) RNA immunoprecipitation (RIP) assay was used to determine RBM38 enrichment at the AR-cryptic exon 3 loci hnRNA (heteronuclear RNA) in 22Rv1 PCa cells at the following loci: 66,831,239-66,840,000 (green), 66,831,239-66,843,000 (red), and 66,917,500-66,920,140 (blue). Cells were treated with vehicle, enzalutamide (5  $\mu$ M/mL), or the combination of enzalutamide and carotuximab (10  $\mu$ g/mL) for 48 h under 2% O<sub>2</sub>. Data were analyzed using two-tailed t test, where statistical significance was indicated: \* $p$  < 0.05, \*\* $p$  < 0.01, \*\*\* $p$  < 0.001, and \*\*\*\* $p$  < 0.0001.

22Rv1 had constitutively high expression of AR-FL, AR-V7, and ID3 that was not affected by BMP2 treatment. Enzalutamide treatment caused an induction of TGF- $\beta$ -responsive PAI-1 and BMP-responsive ID1 in C4-2B cells ( $p$  < 0.0001; Figure S2A). However, enzalutamide reduced PAI-1 expression in wild-type fibroblasts ( $p$  < 0.01) and produce a >2-fold induction of ID1 expression ( $p$  < 0.01). The treatment with enzalutamide and carotuximab in combination or alone did not significantly change AR full-length expression, compared with control (Figure 2C). The upregulation of AR-V7 by enzalutamide was restored to near control levels when combined with carotuximab treatment. The downstream targets of AR-V7, UBE2C and CDC20, were similarly upregulated by enzalutamide ( $p$  < 0.0001) and definitively downregulated by the addition of carotuximab ( $p$  < 0.005; Figures 2C and S2B).<sup>39</sup> Incidentally, the same was not measurable with C4-2B cells, as the combination AR and CD105 antagonism was lethal. Regardless, The Cancer Genome Atlas (TCGA), Jenkins, and Suetlman datasets all demonstrated a significant correlation between AR and CD105 expression in predominantly cancer epithelia (Figure 2D). BMP/CD105 signaling was found to regulate AR RNA splicing events in both cancer epithelia and associated fibroblasts.

### BMP/CD105 regulation of AR splicing and its paracrine influence on PCa ARSI sensitivity

Considering the identification of AR-V7 expression in prostatic CAF, RNA sequencing (RNA-seq) analysis of primary human NAF and CAF lines was used to better understand the mechanism of AR splicing. As RNA-binding proteins are associated with splicing dysregulation of oncogenes,<sup>40,41</sup> we examined differential expression of RNA-binding proteins and AR-regulated genes. We found that RBM15, RBM20, and RBM38 were highly expressed in CAF compared with NAF based on previously reported RNA-seq analysis (Figure 3A).<sup>12</sup> Of the three differentially regulated RNA-binding proteins, RBM38 was found to be downregulated by the combination carotuximab and enzalutamide treatment, below control levels in both CAF and 22Rv1 cells (Figure 3B). These experiments were performed under standard serum-containing media, having an abundance of BMP and TGF- $\beta$  ligands. Carotuximab, however, had little effect on the expression of RBM15 and RBM20 in 22Rv1 and CAF cells (Figure S3A). Based on the strong homology of RBM38 among species, we found that mouse-specific CD105 neutralizing antibody (M1043) treatment reduced the expression of canonical BMP downstream transcription factors ID1 ( $p$  = 0.0380) and ID4 ( $p$  < 0.0001)

expression in wild-type prostatic fibroblasts (Figures S3B and S3C). The knockdown of RBM38 in 22Rv1 reduced the expression of AR-V1 and AR-V7 in a dose-dependent manner, with no apparent effects on the expression of AR-FL or AR-v567es (Figure 3C). Chromatin immunoprecipitation (ChIP) analysis of the RBM38 promoter demonstrated both ID1 and E2F1 loading in 22Rv1 cells (Figure 3D). Carotuximab was found to prevent ID1 binding ( $p = 0.0225$ ) and diminish RNA polymerase II binding to the RBM38 promoter with little effect on E2F1 promoter binding (Figure S3D). Thus, BMP/CD105-mediated ID1 signaling was required for RBM38 expression. Subsequently, we performed an RNA immunoprecipitation (RIP) assay to find that RBM38 is enriched at regions proximal to the AR-cryptic exon 3 under basal conditions (Figure 3E). Enzalutamide treatment of 22Rv1 demonstrated significant RBM38 binding at three loci proximal to cryptic exon 3. However, RBM38 enrichment at the 5' region was nearly 10-fold greater than at the 3' edge of the exon. The addition of carotuximab to enzalutamide restored RBM38 binding to near basal conditions. These results suggested that BMP/CD105 signaling is a mediator of RBM38 expression and contributed to the generation of AR-V7 in both epithelia and fibroblasts.

Next, we wanted to define the role of BMP/CD105 signaling in the mechanism for ARSI sensitivity. Analysis of the Jenkins dataset demonstrated a direct correlation between CD105 and RBM38 expression in PCa patients ( $R = 0.58$ ,  $p = 2.41 \times 10^{-50}$ ) (Figure 4A).<sup>42</sup> However, in enzalutamide-non-responsive subjects, AR had an inverse relationship with RBM38 expression in the SU2C/PCF Dream Team dataset ( $R = -0.86$ ,  $p = 0.0137$ ; Figure 4B).<sup>43</sup> Again, these patients' data correlations were primarily based on prostate tumor epithelia. We tested the differential signaling of CD105 and androgen signaling in models combining prostatic epithelia and fibroblasts. Enzalutamide treatment led to a significant increase in cell-surface CD105 expression by C4-2B when co-cultured with CAF in a Transwell setup ( $p = 0.0296$ ) (Figure 4C). Treatment of 22Rv1 cells with carotuximab and enzalutamide restored AR-V7 expression to near basal levels, with no effect on AR full-length expression. Similarly, M1043 significantly reduced the expression of AR-V2 by mouse prostatic fibroblasts compared with enzalutamide single agent ( $p < 0.01$ ), with little effect on AR-FL (Figure 4D). Enzalutamide and M1043 combination treatment also reduced AR-V2 compared with enzalutamide alone ( $p < 0.05$ ). Previous reports suggested IL-6 induced expression of AR-responsive genes (i.e., *PSA*, *PAI-1*) in androgen-dependent LNCaP PCa cells.<sup>31</sup> We examined the relationship between IL-6 and AR signaling in the context of BMP/CD105 and AR-variant expression. Treating prostatic fibroblasts with mouse-specific IL-6 significantly elevated the expression of AR-FL, AR-V2, as well as RBM38 (Figure S4A). Alternatively, LNCaP-conditioned media-induced elevation of AR-V7 expression in CAF was found to be restored to control levels with IL-6 neutralizing antibody, MAB-206 (Figure 4E). Protein expression of ID1, a CD105 downstream effector, was increased in 22Rv1 after enzalutamide treatment and decreased with MAB-206 or the combination of the two treatments. ID1 mRNA expression was significantly downregulated by MAB-206 in both NAF and LNCaP cells when they were co-cultured

( $p < 0.05$ ). In a co-culture study of LNCaP and CAF, flow cytometry analysis demonstrated cell-surface CD105 expression in both cell lines to be significantly downregulated by MAB-206 (Figure 4F). CAF expression of RBM38 was also downregulated by MAB-206 (Figure 4G). In congruence with past findings, we find that IL-6 mediated the expression of AR-V7/AR-V2; it does so in both prostatic epithelia and fibroblasts (Figure 4H).<sup>30,44</sup> Importantly, targeting paracrine and autocrine IL-6 signaling downregulated CD105 and ID1 signaling in both prostatic fibroblasts and PCa epithelia. These activities enabled RBM38-RNA stabilization to facilitate AR splicing events.

Next, we tested the impact of AR-V7 expression in otherwise non-tumor inductive fibroblasts and the ensuing effects on PCa epithelia. To do so, AR-V7 was exogenously expressed in wild-type mouse prostatic fibroblasts and confirmed by PCR (Figure 5A). AR-V7-expressing fibroblasts were found to express CAF signature genes greater than those transfected with control vector.<sup>10,12</sup> Basal expression of the genes in AR-V7<sup>OE</sup> was similar to wild-type fibroblasts treated with enzalutamide. M1043 diminished CAF gene expression induced by enzalutamide. The epithelial ramifications of fibroblastic AR-V7 and CD105 expression were defined by three-dimensional co-cultures of human PCa epithelia and three primary mouse fibroblasts cultures in a collagen matrix. Enzalutamide and carotuximab treatment decreased Ki67 expression of 22Rv1 cells when co-cultured with wild-type fibroblasts, compared with a negligible inhibition of Ki67 when co-cultured with AR-V7<sup>OE</sup> fibroblasts (Figure 5B). Annexin V staining was higher in 22Rv1 co-cultured with either wild-type fibroblasts or AR-V7<sup>OE</sup> upon treatment of the combination of enzalutamide plus carotuximab. To complement neutralizing antibody studies targeting CD105, we knocked out CD105 in wild-type fibroblasts using CRISPR-Cas9, and subsequently confirmed this by flow cytometry (Figure S4C). Ki67 was decreased in 22Rv1 co-cultured with CD105 knockout (CD105<sup>KO</sup>) fibroblasts treated with enzalutamide and carotuximab in combination, compared with control samples. In addition, enzalutamide caused a significant elevation in epithelial annexin V staining when co-cultured with CD105<sup>KO</sup> fibroblasts, compared with control samples. Parallel studies of tissue recombinants of 22Rv1 and control wild-type or AR-V7<sup>OE</sup> fibroblasts were orthotopically grafted in NOD SCID gamma (NSG) mice and allowed to expand for 6 weeks prior to enzalutamide administration for 4 days prior to sacrifice (Figure 5C). Histologic evaluation of tumor proliferation (phosphorylated-histone H3) and cell death (TUNEL) reflected a similar pattern to that found in co-culture studies, where there was significantly less cell death when AR-V7<sup>OE</sup> fibroblasts were part of the tumors, compared with wild-type fibroblasts ( $p = 0.0469$ ).

#### ARSI/carotuximab combination therapy in patients

To conduct a translational proof of principle, a clinical trial of carotuximab in combination with either abiraterone or enzalutamide was conducted. The trial required that all patients experienced disease progression on ARSI therapy. Details of eligibility are provided in Table S1. While planned for a total of 40 patients, this study was

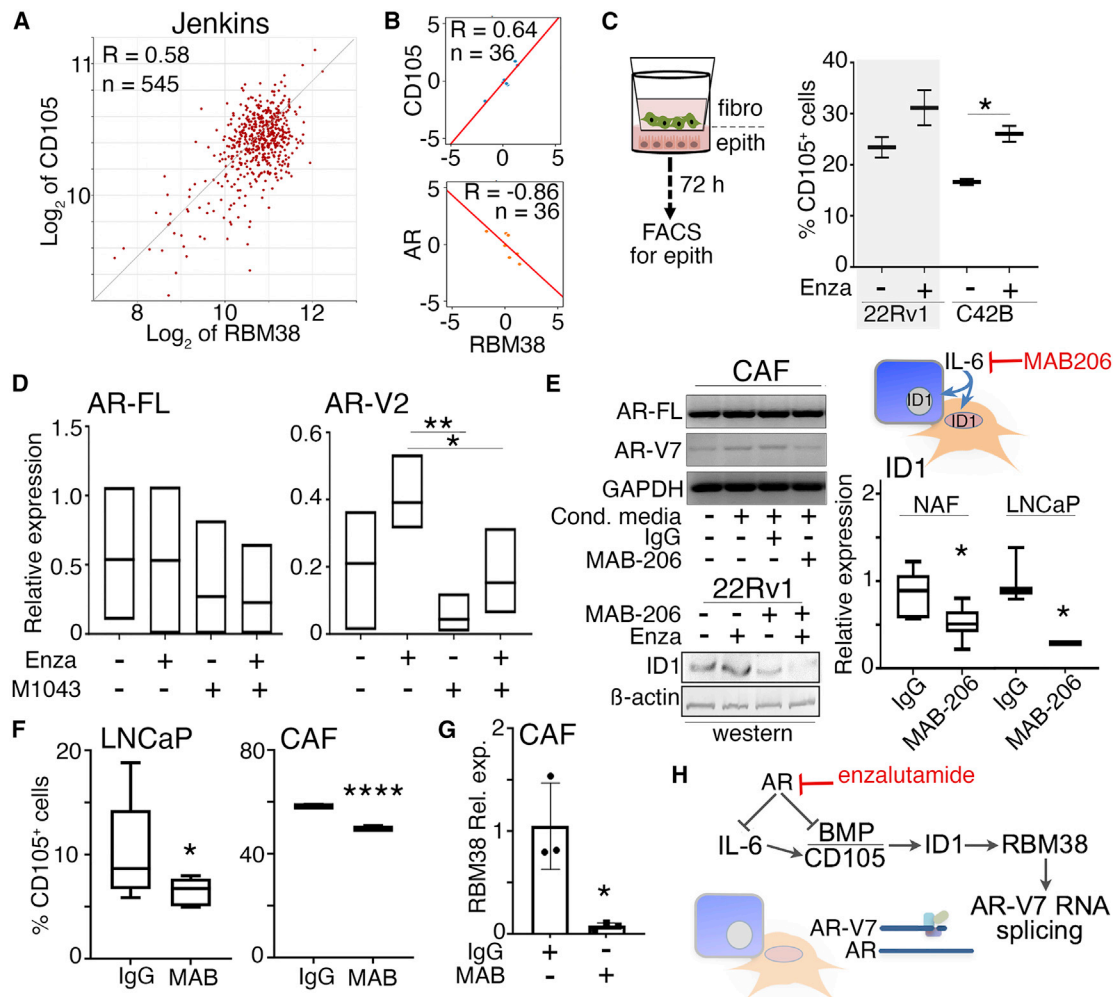


**Figure 4. Androgen and CD105 signaling regulates fibroblastic AR-variant expression**

(A) The Jenkins dataset of PCA patients developing metastatic disease progression demonstrated a correlation between the expression of CD105 and RBM38 ( $p = 2.4 \times 10^{-50}$ ).<sup>42</sup> (B) The Alumkal cohort of metastatic CRPC patients demonstrated a correlation between the expression of CD105 and RBM38 as well as a correlation between RBM38 and AR.<sup>43</sup> The normalized expression values were centered by the mean across all the samples. The x and y axis are the mean centered log<sub>2</sub> transcripts per million relative expression values computed by using Pearson's correlation method. (C) Flow cytometry for cell-surface CD105 was analyzed in 22Rv1 or C4-2B cells co-cultured in Transwells with CAF with indicated treatment for 72 h in 2% O<sub>2</sub>. (D) AR-FL and AR-V2 mRNA expression was measured in wild-type (WT) mouse prostatic fibroblasts following the indicated treatments for 72 h. (E) AR-FL and AR-V7 mRNA expression in human CAFs were measured following 48-h incubation with LNCaP-conditioned media in the presence or absence of MAB-206. Western blot for ID1 expression was visualized in 22Rv1 cells following enzalutamide (Enza) and MAB-206 after 48-h treatment under 2% O<sub>2</sub>. ID1 mRNA expression in both NAF and LNCaP was measured following co-culture with IgG or MAB-206. (F) Cell-surface CD105 was measured in LNCaP and CAFs following treatment with IgG or MAB-206 (MAB) for 48 h at 2% O<sub>2</sub>. (G) RBM38 expression was measured in CAF cells treated with enzalutamide in the presence or absence of MAB-206 for 48 h at 2% O<sub>2</sub>. (H) The data support a mechanism where AR antagonism promotes IL-6 for downstream CD105 signaling in RBM38-mediated AR-V7 generation. Enzalutamide was used at 5 μM, carotuximab 10 μg/mL, M1043 10 μg/mL, MAB-206 150 ng/mL, IgG 10 μg/mL, and DMSO was used as vehicle control. GAPDH was used as loading control for qPCR. Data were analyzed using two-tailed t test, where statistical significance was indicated: \* $p < 0.05$ , \*\* $p < 0.01$ , and \*\*\*\* $p < 0.0001$ .

interrupted by a decision by Tracoon Pharmaceuticals to abandon development of carotuximab due to negative trials in kidney cancer and soft tissue sarcoma. Prior to this decision, 11 patients were accrued. Characteristics of these patients are shown Table 1. Of note, while all patients had at least one prior ARSI, several had up to five clinical interventions prior to enrollment. Two of these patients were not assessable due to rapid disease progression prior

to completion of the loading dose of carotuximab. Adverse events observed were consistent with previous studies of carotuximab.<sup>45,46</sup> Of the assessable patients, the PFS rate at 8 weeks was 44%. Using RECIST 1.1 and PCWG3 criteria, median radiographic PFS was 12 weeks (Figure 6A, range 7–66 weeks). When considering factors related to longer PFS, it became clear that previous lines of therapy affected outcomes: patients with two lines of therapy experienced

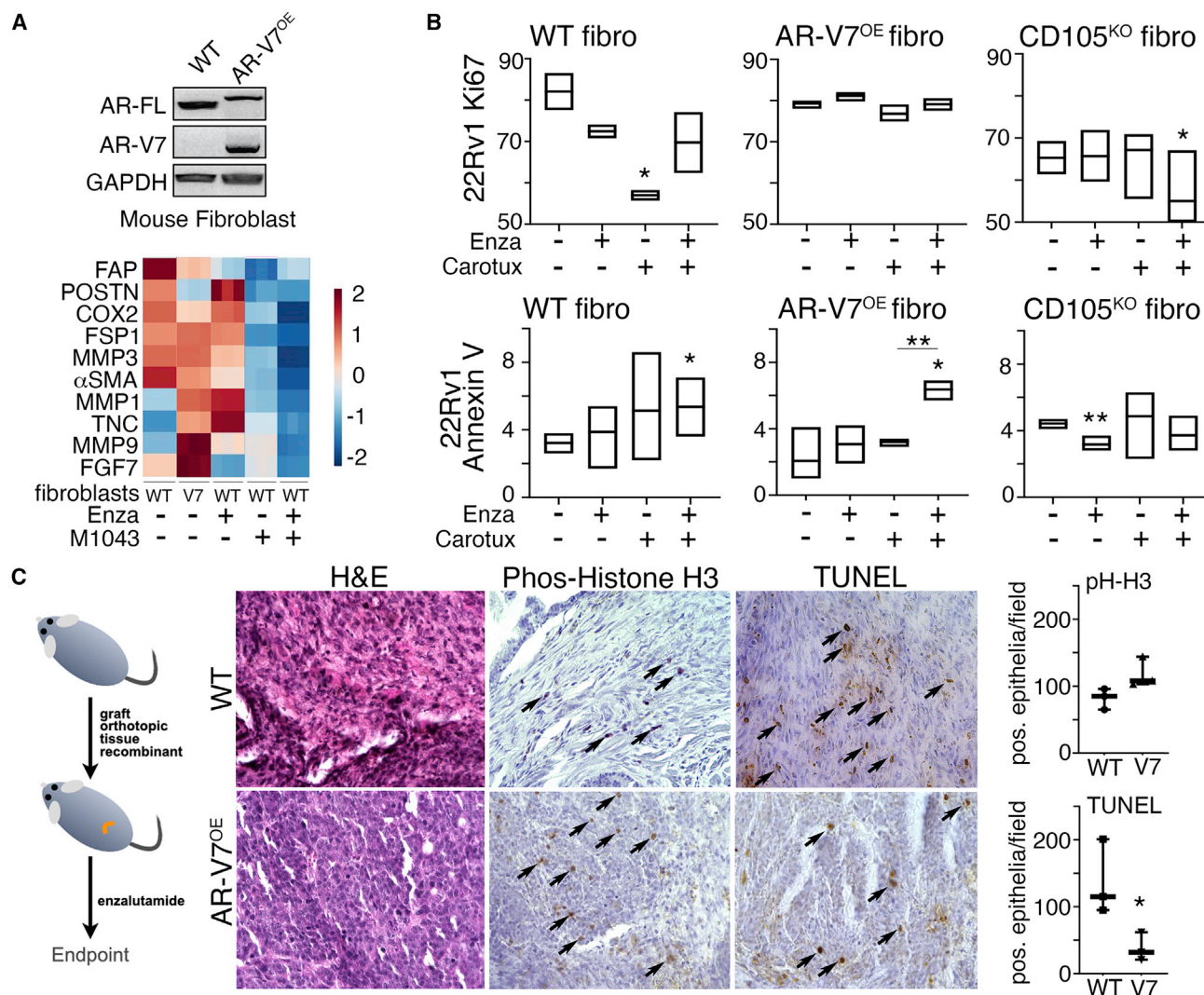


**Figure 5. Fibroblastic AR-V7 expression is consequential to PCa enzalutamide sensitivity**

(A) Overexpression of AR-V7 (AR-V7<sup>OE</sup>) in WT mouse prostatic fibroblasts was validated by RT-PCR and characterized for the expression of CAF marker expression in the presence or absence of enzalutamide and/or M1043 for 72 h. (B) Proliferation of 22Rv1 cells WS measured by flow cytometry for Ki67 following three-dimensional co-cultures with mouse prostatic fibroblasts (WT, AR-V7<sup>OE</sup>, or CD105 knockout [CD105<sup>KO</sup>]) under indicated treatments for 72 h (n = 3). Under the same conditions, apoptosis was measured by annexin V (n = 3). (C) Tissue recombinants of 22Rv1 and mouse prostatic fibroblasts (WT or AR-V7<sup>OE</sup>) were orthotopically grafted and subsequently treated with enzalutamide for 4 days prior to sacrifice. The tumors were evaluated histologically for H&E, and immunohistochemistry (IHC) was used for phosphorylated-histone H3 and TUNEL staining (arrows indicate positive staining). Enzalutamide was used at 5  $\mu$ M in culture or 1 mg/kg in mice, carotuximab at 10  $\mu$ g/mL, M1043 at 10  $\mu$ g/mL, and DMSO used as vehicle control. Data were analyzed using two-tailed t test, where statistical significance was indicated: \*p < 0.05, \*\*p < 0.01.

clinical progression at an average of 52 weeks (range, 32–66 weeks). Among the participants, there were several notable outcomes. One subject (patient 3) with more than five lines of therapy, including docetaxel chemotherapy and stereotactic radiotherapy to brain metastases, experienced a 28% decrease in his serum prostate-specific antigen (PSA) concentration and remained on therapy for 12 weeks before clinical and radiographic progression of his central nervous system (CNS) disease. The two subjects (patients 5 and 10) who remained on therapy the longest (66 and 60 weeks, respectively), had only two lines of therapy and no prior taxane treatment. One of

these patients (patient 10) experienced 3 months of clinical stability after stopping combination therapy. His PSA declined from 18.5 to 4.7 ng/mL before rising to 57.3 ng/mL, at which time he elected to have treatment with a non-steroidal anti-androgen. He had a remarkable biochemical response with a greater than 90% decline in his serum PSA concentration and remained on therapy for 9 months. Of interest, after halting carotuximab therapy, he was taxane responsive and experienced a substantial PSA decline on chemotherapy (57% decrease; PFS, 8 months), despite demonstrating docetaxel resistance in the past. While limited in number,

**Table 1. Summary of patients enrolled and treatment outcomes**

Patient ID	Age (years)	Baseline PSA (ng/mL)	Previous lines of therapy	Previous ARSI	Previous taxane	Best response	PFS (weeks)	Comments
1	72	38.8	3	A/E	no	PD	7	
2	70	728.3	2	A/E	no	NA	NA	unable to complete loading dose
3	57	244.4	5+	A/E	yes	SD	12	PSA decline to 175.3 ng/mL
4	71	11.8	2	A/E	no	PD	7	PSA decline following d/c carotuximab while on enzalutamide
5	72	8.8	2	A/E	no	SD	66	
6	73	2.2	2	E	yes	SD	16	clinical progression at 32 weeks
7	79	182.6	3	A/E	no	PD	7	
8	74	192.3	4	A/E	no	NA		unable to complete 2 weeks
9	75	123.1	5+	A/E	yes	PD	7	
10	74	5.9	2	A	no	SD	60	
11	60	70.5	5	A/E	yes	PD	7	

Prior ARSI therapy included abiraterone (A) and/or enzalutamide (E). Combination therapy achieved progressive disease (PD), stable disease (SD), or not available (NA). The weeks of on-treatment progression-free disease (PFS) are indicated.

The patients enrolled in the NCT03418324 study had multiple lines of prior therapy inclusive of ARSI and taxanes, having progression on either abiraterone or enzalutamide. There were variable responses to the open-label combination therapy strategy of either abiraterone or enzalutamide with carotuximab. Radiographic PFS  $\geq$  8 weeks was a measure response with stable disease.

some patient outcomes appeared to parallel treated mouse models of CRPC.

Gene expression analysis was performed on the circulating tumor cells (CTCs) of the differentially responsive subjects. The pre- and on-treatment patients' blood samples were enriched for CTCs using the NanoVelcro platform.<sup>47</sup> The expression pattern of genes, previously described to define PCa outcome, were measured by a custom NanoString gene panel curated based on the PCS (Prostate Cancer Classification System) and PAM50 subtyping classification systems.<sup>48,49</sup> ARG2, CSRP1, and KIAA1324 were identified from blood collected prior to treatment having responsivity to the combination therapy, based on Z score (Table S2; Figure S5A).<sup>50</sup> Human genome data obtained from the Bittner dataset demonstrated that these three markers were highly expressed in PCa compared with 15 other cancer types (Figure S5B). Furthermore, expression of KIAA1324 was similarly expressed in only breast, esophageal, and pancreatic cancers compared with PCa. From our clinical samples, pre-treatment CTC markers differentiated the responsive patients from the non-responsive subjects with a significant combined Z score. In further validating the model systems used, we found that the gene expression patterns observed clinically for CSRP1, KIAA1324, and ARG2 could be recapitulated in cultured 22Rv1 cells (Figure 6C). As a point of reference, two PCa lineage plasticity markers, NKX2.2 and SCG3, followed a similar induction pattern as CSRP1, KIAA1324, and ARG2 following enzalutamide or enzalutamide and carotuximab combination. However, examining gene expression in the CTCs on treatment differentiated the patients responsive to the ARSI/carotuximab combination treatment from those not responsive through several differentially expressed genes (Table S2). In particular, the expression of AR-V7 (AR-CE3) and downstream gene, CDC20, were significantly downregulated by combination ther-

apy in responsive patients, as identified in pre-clinical studies (Figure S2E).

## DISCUSSION

Intensive AR signaling suppression is part of advanced PCa patient standard of care, primarily utilized to treat CRPC. Not surprisingly, ARSIs have greater efficacy in castration-sensitive patients. However, ARSI treatment seemed to promote AR-V7 expression in both cancer epithelia and CAF populations by autocrine and paracrine BMP signaling (Figures 1 and 2). The epigenetic loss of *Tgfb2* expression in CAF has previously been reported.<sup>51</sup> Here, we demonstrated that this loss in TGF- $\beta$  signaling, similarly achieved by the expression of CD105, can promote AR-V7 expression. The upregulation of CD105 expression by enzalutamide was associated with epithelial-derived BMP ligand expression. Both the loss of Smad2/3 signaling downstream of TGF- $\beta$  signaling and the gain of BMP signaling cause the common induction of ID transcriptional activity.<sup>52,53</sup> Accordingly, we found AR-V7 to be downregulated by CD105 neutralizing antibodies, carotuximab, and M1043 in respective human and mouse cells. Given these considerations, an inhibitor of AR-V7 expression that also downregulates paracrine mediators of tumor progression represents a significant advance in the use of ARSI therapies.<sup>12</sup> ARSIs are being deployed during PCa progression, and the observed elevation of BMP ligands and CD105 signaling further the importance of AR-V7 regulators such as RBM38 (Figure 3). Specifically, BMP/CD105-dependent ID1 loading on the RBM38 promoter was necessary for its transcription. The extensive study of AR-V7 thus far had not revealed the RNA-binding proteins responsible, despite the recognized importance of the splicing event. The direct interaction of RBM38 in response to ARSI with the AR-cryptic exon 3 was evidence of its role in AR splicing, potentially through RNA stabilization.<sup>54</sup> RBM38 is reported to have

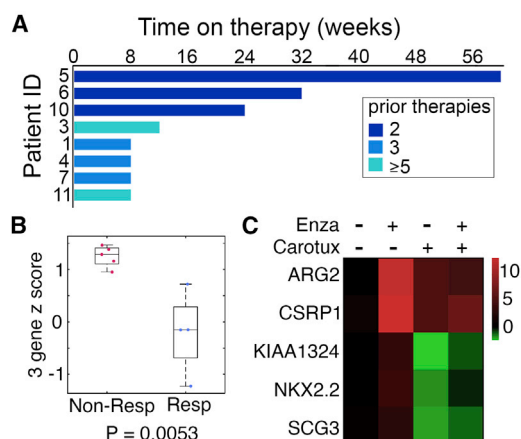


**Figure 6. Targeted androgen and CD105 inhibition combination therapy were evaluated in patients**

(A) The time on combination therapy is indicated with relation to the number of clinical interventions prior to accrual to the phase 2 clinical trial for the individual patients. (B) CTC enrichment in patients revealed differentially expressed pre-treatment markers, ARG2, CSRP1, and KIAA1324; when combined, they distinguish non-responsive and responsive subjects. (C) 22Rv1 cells treated with enzalutamide (Enza), carotuximab (Carotux), or the combination for 72 h at 2% O<sub>2</sub> were evaluated by RT-PCR. Enzalutamide was used at 5 μM, carotuximab 10 μg/mL, and DMSO used as vehicle control. Data were analyzed using two-ANOVA, where statistical significance was indicated.

opposing tumor-suppressive and -promoting functions during cancer development. Here, the ARSI-induced RBM38 expression seems to serve as a means of therapy resistance.

There was a similarity between the mechanism of ARSI-induced AR-V7 expression in stromal fibroblasts and PCa cells. Despite the consistency of AR-V7 expression, other AR splice variants appear to differ in expression levels among the prostatic NAF, CAF, and PCa cell lines examined. The parallels in the mechanism of AR-V7 expression were supported by the strong mechanistic connection between CD105 and RBM38 expression we revealed in prostatic CAF and PCa cells (Figures 3 and 4). The consequence of fibroblastic AR-V7 expression by its overexpression in mouse prostatic fibroblasts was its support of epithelial resistance to enzalutamide treatment in a paracrine manner (Figure 5). Based on the established role of IL-6 in AR-V7 expression, the observation that CD105, ID1, and RBM38 were downstream mediators of IL-6 provided a mechanistic detail missing thus far (Figure S4). Other cancers, such as bladder, liver, kidney, lung, and breast, also express AR, but the narrow use of ARSI treatment limits splice variant expression in these tissues.<sup>55,56</sup> However, the role of AR splice variant expression by fibroblasts of PCa secondary metastatic sites, such as the bone, lung, and liver, may have a greater role in ARSI responsiveness than originally realized.

The interventional clinical trial testing the viability of combining carotuximab with enzalutamide or abiraterone was the first time stromal fibroblasts and epithelial cells were targeted simultaneously to treat PCa. Despite the unexpected trial closure due to unavailability of car-

otuximab, the nine assessable subjects demonstrated viability of the combination therapy strategy. While the subjects were generally heavily pretreated, three of the four patients that demonstrated favorable PFS only had two treatment modalities prior to accrual to the trial (Figure 6). Safety concerns with this combination therapy primarily involved infusion reactions as well as epistaxis and anemia requiring close management. Considering the heterogeneity of response, there may be a benefit in a biomarker-selected population, such as the expression signature found in CTCs enriched before treatment. Indeed, the downregulation of AR-V7 and its downstream target, CDC20, for the patients on combination therapy distinguished the responders from the non-responders. Although the gene expressions in the CAFs of these patients remain unknown, the analogous AR-V7 regulation in both cell compartments preclinically would suggest the concomitant downregulation of AR-V7 in the CAF of the treatment responders. Importantly, the pre-treatment level of AR-V7 expression was not distinguished in treatment responders. The genes differentially expressed in the responder population were validated in cultured cells upon combination treatment. The three-gene panel that identified responsive subjects prior to treatment had the caveat of the small patient number. In conclusion, antagonizing CD105 with AR in pre-clinical models and patients increased therapeutic benefit. We demonstrated ARSIs upregulate AR-V7 expression in PCa cells and associated fibroblasts in a CD105-dependent manner. Carotuximab does not induce an antibody-dependent cytotoxicity response on its own, but supports a synthetic lethality strategy when combined with ARSI.

## MATERIALS AND METHODS

### Animal studies

All animal procedures were performed according to an approved protocol from the Institutional Animal Care and Use Committee at Cedars-Sinai Medical Center (IACUC007440). Male NSG, 8–10 weeks old, were used for prostatic orthotopic grafting, respectively, as previously described.<sup>51</sup> For PDX models, and in accordance with institutional animal care and use committee approval, prostatectomy tissues were xenografted into the sub-renal capsules and mice were treated for 4 days with enzalutamide (1 mg per mouse by oral gavage), dimethyl sulfoxide (DMSO) was used as vehicle control. In accordance with institutional animal care and use committee approval,  $3 \times 10^5$  22Rv1 cells and  $9 \times 10^5$  mouse prostatic fibroblasts (wild type or AR-V7<sup>OE</sup>) were suspended in 30–50 μL of type I collagen and grafted into the anterior prostate. Tumor volume was calculated using the modified ellipsoid formula  $\text{volume}^3 = \pi/6 \times (\text{width})^2 \times \text{length}$ . Attrition was controlled by implanting each mouse with two grafts containing  $1.2 \times 10^6$  cells per graft. Mice were returned to cages with littermates after survival surgeries. Tumors grew for 4 weeks, followed by euthanasia and tissue analysis. There was blinding of this experiment because, although all mice were treated the same, the tumor sizes prior to treatment were unknown. For power analysis, an adequate sample size was used because there were five mice used per group. The number of mice per group needed to conduct the experiment was five, although seven were used to control for attrition or unforeseen complications.

### Patients and study design

This was a single-institution, open-label, phase 2 study (ClinicalTrials.gov identifier NCT03418324) that consisted of two parallel treatment arms defined by the treatment given in concert with carotuximab with either abiraterone or enzalutamide. Eligible patients had history of CRPC with biochemical progression (i.e., rising serum PSA concentration) and radiographic progression on either abiraterone or enzalutamide. Detailed eligibility criteria are found in Table S1. Patients who were on active therapy with an abiraterone or enzalutamide were required to hold treatment for 2 weeks prior to starting combination therapy. Patients were required to restart the ARSI on which they progressed in combination with carotuximab. The study was designed to accrue in the two arms independently. There were no limits on prior therapy and previous chemotherapy was allowed. Patients were >18 years of age and had a life expectancy of >3 months. ECOG (Eastern Cooperative Oncology Group) performance status was required to be 2 or better. Patients were required to have normal organ function including platelets >60,000/ $\mu$ L, 8.5 g/dL hemoglobin, and serum creatinine <1.5 $\times$  upper limit of normal. Patients with non-PSA-producing tumors or those that progress without increasing serum PSA concentration were excluded. Patients with uncontrolled hypertension and those unable to tolerate full standard doses of abiraterone or enzalutamide were also excluded. Full eligibility criteria are presented in the [supplemental information](#). Per the manufacturer's recommendations, carotuximab therapy was initiated using a 4-week loading period: 3 mg/kg days 1 and 4 then 10 mg/kg on days 8, 15, and 21. Starting at cycle 2, carotuximab was administered as a 15-mg/kg infusion every 2 weeks. Cycles were 28 days in duration. It was determined that 20 patients per arm would have been adequate to determine the effectiveness of the planned combinations.

This study was conducted in accordance with the guidelines of Good Clinical Practice (defined by the International Council on Harmonization) and the principles of the Declaration of Helsinki. The protocol was reviewed and approved by the Cedars-Sinai Medical Center (CSMC) Institutional Review Board (Pro00048207). All patients provided written informed consent in accordance with CSMC policies.

### Study endpoints and procedures

Clinical and biochemical assessments were made every 4 weeks. Radiographic assessments were obtained every 8 weeks. The primary endpoint of this study was clinical benefit rate (CBR), defined as stabilization of disease for at least 2 months or improvement at any time from the start of combination therapy by radiographic and/or biochemical criteria. Biochemical and radiographic response data were assessed using Prostate Cancer Clinical Trials Working Group 3 (PCWG3)<sup>57</sup> and/or Response Evaluation Criteria in Solid Tumors (RECIST 1.1) criteria.<sup>58</sup> Secondary endpoints included assessment of grade 3–4 toxicity using Common Terminology Criteria for Adverse Events (CTCAE) 4.0, PFS, and CBR at 2 and 4 months. See [supplemental information](#) for additional methods.

### DATA AND CODE AVAILABILITY

The data that support the findings of this study are available from the corresponding author on reasonable request.

### SUPPLEMENTAL INFORMATION

Supplemental information can be found online at <https://doi.org/10.1016/j.ymthe.2022.08.019>.

### ACKNOWLEDGMENTS

We would like to thank the patients, families, and caregivers who participated in the trial. This work was supported by the Department of Defense (W81XWH-17-1-0154 to BS), National Cancer Institute (CA233452 to N.A.B. and E.M.P.), and Veterans Administration (I01BX001040 to N.A.B.).

The funding agencies did not influence the design or outcomes of the study.

### AUTHOR CONTRIBUTIONS

B.S., conceptualization, data curation, formal analysis, investigation, methodology, validation, writing – original draft, and review & editing; R.M., conceptualization, data curation, and formal analysis; S.B., methodology, formal analysis, and validation; V.P., methodology and validation; M.K., formal analysis; L.Z., formal analysis; F.D., data collection; A.M., data curation; K.S., data collection; N.M., data collection and curation; A.O., data collection and curation; B.A., data collection; S.Y., formal analysis and writing – review & editing; M.T., data curation and writing – review & editing; E.M.P., conceptualization, data curation, formal analysis, and writing – review & editing; N.A.B., conceptualization, formal analysis, and writing – review & editing.

### DECLARATION OF INTERESTS

B.S. and N.A.B. have filed patents on the application of carotuximab. N.A.B. has >10% ownership of Kairos Pharma, Ltd., distributor of carotuximab.

### REFERENCES

1. Siegel, R.L., Miller, K.D., Fuchs, H.E., and Jemal, A. (2021). Cancer statistics, 2021. *CA. Cancer J. Clin.* 71, 7–33.
2. Negoita, S., Feuer, E.J., Mariotto, A., Cronin, K.A., Petkov, V.I., Hussey, S.K., Benard, V., Henley, S.J., Anderson, R.N., Fedewa, S., et al. (2018). Annual Report to the Nation on the Status of Cancer, part II: recent changes in prostate cancer trends and disease characteristics. *Cancer* 124, 2801–2814.
3. Kahn, B., Collazo, J., and Kyprianou, N. (2014). Androgen receptor as a driver of therapeutic resistance in advanced prostate cancer. *Int. J. Biol. Sci.* 10, 588–595.
4. Crona, D.J., Milowsky, M.I., and Whang, Y.E. (2015). Androgen receptor targeting drugs in castration-resistant prostate cancer and mechanisms of resistance. *Clin. Pharmacol. Ther.* 98, 582–589.
5. Antonarakis, E.S., Lu, C., Wang, H., Lubner, B., Nakazawa, M., Roeser, J.C., Chen, Y., Mohammad, T.A., Chen, Y., Fedor, H.L., et al. (2014). AR-V7 and resistance to enzalutamide and abiraterone in prostate cancer. *N. Engl. J. Med.* 371, 1028–1038.
6. Beer, T.M., Armstrong, A.J., Rathkopf, D.E., Loriot, Y., Sternberg, C.N., Higano, C.S., Iversen, P., Bhattacharya, S., Carles, J., Chowdhury, S., et al. (2014). Enzalutamide in metastatic prostate cancer before chemotherapy. *N. Engl. J. Med.* 371, 424–433.

7. Scher, H.I., Fizazi, K., Saad, F., Taplin, M.E., Sternberg, C.N., Miller, K., de Wit, R., Mulders, P., Chi, K.N., Shore, N.D., et al. (2012). Increased survival with enzalutamide in prostate cancer after chemotherapy. *N. Engl. J. Med.* 367, 1187–1197.
8. Yu, Z., Chen, S., Sowalsky, A.G., Voznesensky, O.S., Mostaghel, E.A., Nelson, P.S., Cai, C., and Balk, S.P. (2014). Rapid induction of androgen receptor splice variants by androgen deprivation in prostate cancer. *Clin. Cancer Res.* 20, 1590–1600.
9. Placencio, V.R., Sharif-Afshar, A.R., Li, X., Huang, H., Uwamariya, C., Neilson, E.G., Shen, M.M., Matusik, R.J., Hayward, S.W., and Bhowmick, N.A. (2008). Stromal transforming growth factor-beta signaling mediates prostatic response to androgen ablation by paracrine Wnt activity. *Cancer Res.* 68, 4709–4718.
10. Mishra, R., Haldar, S., Placencio, V., Madhav, A., Rohena-Rivera, K., Agarwal, P., Duong, F., Angara, B., Tripathi, M., Liu, Z., et al. (2018). Stromal epigenetic alterations drive metabolic and neuroendocrine prostate cancer reprogramming. *J. Clin. Invest.* 128, 4472–4484.
11. Li, X., Placencio, V., Iturregui, J.M., Uwamariya, C., Sharif-Afshar, A.R., Koyama, T., Hayward, S.W., and Bhowmick, N.A. (2008). Prostate tumor progression is mediated by a paracrine TGF-beta/Wnt3a signaling axis. *Oncogene* 27, 7118–7130.
12. Kato, M., Placencio-Hickok, V.R., Madhav, A., Haldar, S., Tripathi, M., Billet, S., Mishra, R., Smith, B., Rohena-Rivera, K., Agarwal, P., et al. (2019). Heterogeneous cancer-associated fibroblast population potentiates neuroendocrine differentiation and castrate resistance in a CD105-dependent manner. *Oncogene* 38, 716–730.
13. Thalmann, G.N., Rhee, H., Sikes, R.A., Pathak, S., Multani, A., Zhou, H.E., Marshall, F.F., and Chung, L.W.K. (2010). Human prostate fibroblasts induce growth and confer castration resistance and metastatic potential in LNCaP Cells. *Eur. Urol.* 58, 162–171.
14. Qi, J., Tripathi, M., Mishra, R., Sahgal, N., Fazli, L., Fazli, L., Ettinger, S., Placzek, W.J., Claps, G., Chung, L.W.K., et al. (2013). The E3 ubiquitin ligase Siah2 contributes to castration-resistant prostate cancer by regulation of androgen receptor transcriptional activity. *Cancer Cell* 23, 332–346.
15. Olumi, A.F., Grossfeld, G.D., Hayward, S.W., Carroll, P.R., Tlsty, T.D., and Cunha, G.R. (1999). Carcinoma-associated fibroblasts direct tumor progression of initiated human prostatic epithelium. *Cancer Res.* 59, 5002–5011.
16. Hayward, S.W., Wang, Y., Cao, M., Hom, Y.K., Zhang, B., Grossfeld, G.D., Sudilovsky, D., and Cunha, G.R. (2001). Malignant transformation in a nontumorigenic human prostatic epithelial cell line. *Cancer Res.* 61, 8135–8142.
17. Song, B., Park, S.H., Zhao, J.C., Fong, K.W., Li, S., Lee, Y., Yang, Y.A., Sridhar, S., Lu, X., Abdulkadir, S.A., et al. (2019). Targeting FOXA1-mediated repression of TGF-beta signaling suppresses castration-resistant prostate cancer progression. *J. Clin. Invest.* 129, 569–582.
18. Kyprianou, N., and Isaacs, J.T. (1989). Expression of transforming growth factor-beta in the rat ventral prostate during castration-induced programmed cell death. *Mol. Endocrinol.* 3, 1515–1522.
19. Guo, Y., and Kyprianou, N. (1999). Restoration of transforming growth factor beta signaling pathway in human prostate cancer cells suppresses tumorigenicity via induction of caspase-1-mediated apoptosis. *Cancer Res.* 59, 1366–1371.
20. Kiskowski, M.A., Jackson, R.S., 2nd, Banerjee, J., Li, X., Kang, M., Iturregui, J.M., Franco, O.E., Hayward, S.W., and Bhowmick, N.A. (2011). Role for stromal heterogeneity in prostate tumorigenesis. *Cancer Res.* 71, 3459–3470.
21. Barbara, N.P., Wrana, J.L., and Letarte, M. (1999). Endoglin is an accessory protein that interacts with the signaling receptor complex of multiple members of the transforming growth factor-beta superfamily. *J. Biol. Chem.* 274, 584–594.
22. Goumans, M.J., Liu, Z., and ten Dijke, P. (2009). TGF-beta signaling in vascular biology and dysfunction. *Cell Res.* 19, 116–127.
23. Li, D.Y., Sorensen, L.K., Brooke, B.S., Urness, L.D., Davis, E.C., Taylor, D.G., Boak, B.B., and Wendel, D.P. (1999). Defective angiogenesis in mice lacking endoglin. *Science* 284, 1534–1537.
24. Nolan-Stevaux, O., Zhong, W., Culp, S., Shaffer, K., Hoover, J., Wickramasinghe, D., and Ruefli-Brasse, A. (2012). Endoglin requirement for BMP9 signaling in endothelial cells reveals new mechanism of action for selective anti-endoglin antibodies. *PLoS One* 7, e50920.
25. Karzai, F.H., Apolo, A.B., Cao, L., Madan, R.A., Adelberg, D.E., Parnes, H., McLeod, D.G., Harold, N., Peer, C., Yu, Y., et al. (2015). A phase I study of TRC105 anti-endoglin (CD105) antibody in metastatic castration-resistant prostate cancer. *BJU Int.* 116, 546–555.
26. Duffy, A.G., Ulahannan, S.V., Cao, L., Rahma, O.E., Makarova-Rusher, O.V., Kleiner, D.E., Fioravanti, S., Walker, M., Carey, S., Yu, Y., et al. (2015). A phase II study of TRC105 in patients with hepatocellular carcinoma who have progressed on sorafenib. *United Eur. Gastroenterol. J.* 3, 453–461.
27. Wu, H.W., Sheard, M.A., Malvar, J., Fernandez, G.E., DeClerck, Y.A., Blavier, L., Shimada, H., Theuer, C.P., Sposto, R., and Seeger, R.C. (2019). Anti-CD105 antibody eliminates tumor microenvironment cells and enhances anti-GD2 antibody immunotherapy of neuroblastoma with activated natural killer cells. *Clin. Cancer Res.* 25, 4761–4774.
28. Schoonderwoerd, M.J.A., Koops, M.F.M., Angela, R.A., Koolmoes, B., Toitou, M., Paaue, M., Barnhoorn, M.C., Liu, Y., Sier, C.F.M., Hardwick, J.C.H., et al. (2020). Targeting endoglin-expressing regulatory T cells in the tumor microenvironment enhances the effect of PD1 checkpoint inhibitor immunotherapy. *Clin. Cancer Res.* 26, 3831–3842.
29. Li, Y., Xie, N., Gleave, M.E., Rennie, P.S., and Dong, X. (2015). AR-v7 protein expression is regulated by protein kinase and phosphatase. *Oncotarget* 6, 33743–33754.
30. Lin, D.L., Whitney, M.C., Yao, Z., and Keller, E.T. (2001). Interleukin-6 induces androgen responsiveness in prostate cancer cells through up-regulation of androgen receptor expression. *Clin. Cancer Res.* 7, 1773–1781.
31. Chen, T., Wang, L.H., and Farrar, W.L. (2000). Interleukin 6 activates androgen receptor-mediated gene expression through a signal transducer and activator of transcription 3-dependent pathway in LNCaP prostate cancer cells. *Cancer Res.* 60, 2132–2135.
32. de Wit, R., de Bono, J., Sternberg, C.N., Fizazi, K., Tombal, B., Wülfing, C., Kramer, G., Eymard, J.C., Bamias, A., Carles, J., et al. (2019). Cabazitaxel versus abiraterone or enzalutamide in metastatic prostate cancer. *N. Engl. J. Med.* 381, 2506–2518.
33. Corn, P.G., Heath, E.L., Zurita, A., Ramesh, N., Xiao, L., Sei, E., Li-Ning-Tapia, E., Tu, S.M., Subudhi, S.K., Wang, J., et al. (2019). Cabazitaxel plus carboplatin for the treatment of men with metastatic castration-resistant prostate cancers: a randomised, open-label, phase 1-2 trial. *Lancet Oncol.* 20, 1432–1443.
34. Hoskin, P., Sartor, O., O'Sullivan, J.M., Johannessen, D.C., Helle, S.I., Logue, J., Bottomley, D., Nilsson, S., Vogelzang, N.J., Fang, F., et al. (2014). Efficacy and safety of radium-223 dichloride in patients with castration-resistant prostate cancer and symptomatic bone metastases, with or without previous docetaxel use: a prespecified subgroup analysis from the randomised, double-blind, phase 3 ALSYMPCA trial. *Lancet Oncol.* 15, 1397–1406.
35. Sartor, O., de Bono, J., Chi, K.N., Fizazi, K., Herrmann, K., Rahbar, K., Tagawa, S.T., Nordquist, L.T., Vaishampayan, N., El-Haddad, G., et al. (2021). Lutetium-177-PSMA-617 for metastatic castration-resistant prostate cancer. *N. Engl. J. Med.* 385, 1091–1103.
36. Antonarakis, E.S., Lu, C., Luber, B., Wang, H., Chen, Y., Zhu, Y., Silberstein, J.L., Taylor, M.N., Maughan, B.L., Denmeade, S.R., et al. (2017). Clinical significance of androgen receptor splice variant-7 mRNA detection in circulating tumor cells of men with metastatic castration-resistant prostate cancer treated with first- and second-line abiraterone and enzalutamide. *J. Clin. Oncol.* 35, 2149–2156.
37. Sharp, A., Coleman, I., Yuan, W., Sprenger, C., Dolling, D., Rodrigues, D.N., Russo, J.W., Figueiredo, I., Bertan, C., Seed, G., et al. (2019). Androgen receptor splice variant-7 expression emerges with castration resistance in prostate cancer. *J. Clin. Invest.* 129, 192–208.
38. Ning, J., Zhao, Y., Ye, Y., and Yu, J. (2019). Opposing roles and potential antagonistic mechanism between TGF-beta and BMP pathways: implications for cancer progression. *EBioMedicine* 41, 702–710.
39. Yang, Y.C., Banuelos, C.A., Mawji, N.R., Wang, J., Kato, M., Haile, S., McEwan, I.J., Plymate, S., and Sadar, M.D. (2016). Targeting androgen receptor activation function-1 with EPI to overcome resistance mechanisms in castration-resistant prostate cancer. *Clin. Cancer Res.* 22, 4466–4477.
40. Zou, C., Wan, Y., He, L., Zheng, J.H., Mei, Y., Shi, J., Zhang, M., Dong, Z., and Zhang, D. (2020). RBM38 in cancer: role and mechanism. *Cell Mol. Life Sci.* 78, 117–128.
41. Qin, H., Ni, H., Liu, Y., Yuan, Y., Xi, T., Li, X., and Zheng, L. (2020). RNA-binding proteins in tumor progression. *J. Hematol. Oncol.* 13, 90.

42. Erho, N., Crisan, A., Vergara, I.A., Mitra, A.P., Ghadessi, M., Buerki, C., Bergstrahl, E.J., Kollmeyer, T., Fink, S., Haddad, Z., et al. (2013). Discovery and validation of a prostate cancer genomic classifier that predicts early metastasis following radical prostatectomy. *PLoS One* 8, e66855.
43. Alumkal, J.J., Sun, D., Lu, E., Beer, T.M., Thomas, G.V., Latour, E., Aggarwal, R., Cetnar, J., Ryan, C.J., Tabatabaei, S., et al. (2020). Transcriptional profiling identifies an androgen receptor activity-low, stemness program associated with enzalutamide resistance. *Proc. Natl. Acad. Sci. USA* 117, 12315–12323.
44. Lee, S.O., Lou, W., Hou, M., de Miguel, F., Gerber, L., and Gao, A.C. (2003). Interleukin-6 promotes androgen-independent growth in LNCaP human prostate cancer cells. *Clin. Cancer Res.* 9, 370–376.
45. Choueiri, T.K., Zakharia, Y., Pal, S., Kocsis, J., Pachynski, R., Poprach, A., Nixon, A.B., Liu, Y., Starr, M., Lyu, J., et al. (2021). Clinical results and biomarker analyses of axitinib and TRC105 versus axitinib alone in patients with advanced or metastatic renal cell carcinoma (TRAXAR). *Oncologist* 26, 560–e1103.
46. Mehta, C.R., Liu, L., and Theuer, C. (2019). An adaptive population enrichment phase III trial of TRC105 and pazopanib versus pazopanib alone in patients with advanced angiosarcoma (TAPPAS trial). *Ann. Oncol.* 30, 103–108.
47. Chen, J.F., Ho, H., Lichterman, J., Lu, Y.T., Zhang, Y., Garcia, M.A., Chen, S.F., Liang, A.J., Hodara, E., Zhou, H.E., et al. (2015). Subclassification of prostate cancer circulating tumor cells by nuclear size reveals very small nuclear circulating tumor cells in patients with visceral metastases. *Cancer* 121, 3240–3251.
48. You, S., Knudsen, B.S., Erho, N., Alshalalfa, M., Takhar, M., Al-Deen Ashab, H., Davicioni, E., Karnes, R.J., Klein, E.A., Den, R.B., et al. (2016). Integrated classification of prostate cancer reveals a novel luminal subtype with poor outcome. *Cancer Res.* 76, 4948–4958.
49. Zhao, S.G., Chang, S.L., Erho, N., Yu, M., Lehrer, J., Alshalalfa, M., Speers, C., Cooperberg, M.R., Kim, W., Ryan, C.J., et al. (2017). Associations of luminal and basal subtyping of prostate cancer with prognosis and response to androgen deprivation therapy. *JAMA Oncol.* 3, 1663–1672.
50. Rhodes, D.R., Yu, J., Shanker, K., Deshpande, N., Varambally, R., Ghosh, D., Barrette, T., Pandey, A., and Chinnaiyan, A.M. (2004). ONCOMINE: a cancer microarray database and integrated data-mining platform. *Neoplasia* 6, 1–6.
51. Banerjee, J., Mishra, R., Li, X., Jackson, R.S., 2nd, Sharma, A., and Bhowmick, N.A. (2014). A reciprocal role of prostate cancer on stromal DNA damage. *Oncogene* 33, 4924–4931.
52. Ganapathy, A., Paterson, I.C., Prime, S.S., Eveson, J.W., Pring, M., Price, N., Threadgold, S.P., and Davies, M. (2010). TGF-beta inhibits metastasis in late stage human squamous cell carcinoma of the skin by a mechanism that does not involve Id1. *Cancer Lett.* 298, 107–118.
53. Ogata, T., Wozney, J.M., Benezra, R., and Noda, M. (1993). Bone morphogenetic protein 2 transiently enhances expression of a gene, Id (inhibitor of differentiation), encoding a helix-loop-helix molecule in osteoblast-like cells. *Proc. Natl. Acad. Sci. USA* 90, 9219–9222.
54. Zhang, J., Xu, E., Ren, C., Yan, W., Zhang, M., Chen, M., Cardiff, R.D., Imai, D.M., Wisner, E., and Chen, X. (2014). Mice deficient in Rbm38, a target of the p53 family, are susceptible to accelerated aging and spontaneous tumors. *Proc. Natl. Acad. Sci. USA* 111, 18637–18642.
55. Hu, D.G., Hickey, T.E., Irvine, C., Wijayakumara, D.D., Lu, L., Tilley, W.D., Selth, L.A., and Mackenzie, P.I. (2014). Identification of androgen receptor splice variant transcripts in breast cancer cell lines and human tissues. *Horm. Cancer* 5, 61–71.
56. Chang, C., Lee, S.O., Yeh, S., and Chang, T.M. (2014). Androgen receptor (AR) differential roles in hormone-related tumors including prostate, bladder, kidney, lung, breast and liver. *Oncogene* 33, 3225–3234.
57. Scher, H.I., Morris, M.J., Stadler, W.M., Higano, C., Basch, E., Fizazi, K., Antonarakis, E.S., Beer, T.M., Carducci, M.A., Chi, K.N., et al. (2016). Trial design and objectives for castration-resistant prostate cancer: updated recommendations from the prostate cancer clinical trials working group 3. *J. Clin. Oncol.* 34, 1402–1418.
58. Eisenhauer, E.A., Therasse, P., Bogaerts, J., Schwartz, L.H., Sargent, D., Ford, R., Dancey, J., Arbuck, S., Gwyther, S., Mooney, M., et al. (2009). New response evaluation criteria in solid tumours: revised RECIST guideline (version 1.1). *Eur. J. Cancer* 45, 228–247.